

9138

NACA TN 2780

0065864



TECH LIBRARY KAFB, NM

# NATIONAL ADVISORY COMMITTEE FOR AERONAUTICS

TECHNICAL NOTE 2780

FLIGHT INVESTIGATION OF TRANSIENT WING RESPONSE ON A  
FOUR-ENGINE BOMBER AIRPLANE IN ROUGH AIR WITH  
RESPECT TO CENTER-OF-GRAVITY ACCELERATIONS

By Harry C. Mickelboro, Richard B. Fahrer,  
and C. C. Shufflebarger

Langley Aeronautical Laboratory  
Langley Field, Va.



Washington  
September 1952

AFM 1  
TECHNICAL LIBRARY  
AFL 2811



## NATIONAL ADVISORY COMMITTEE FOR AERONAUTICS

## TECHNICAL NOTE 2780

FLIGHT INVESTIGATION OF TRANSIENT WING RESPONSE ON A  
FOUR-ENGINE BOMBER AIRPLANE IN ROUGH AIR WITH  
RESPECT TO CENTER-OF-GRAVITY ACCELERATIONS

By Harry C. Mickleboro, Richard B. Fahrer,  
and C. C. Shufflebarger

## SUMMARY

In continuation of flight studies of transient wing response initiated on a two-engine transport airplane, a flight investigation was undertaken on a four-engine bomber airplane to determine the effect of transient wing response in rough air upon acceleration measurements at the center of gravity of the airplane. Flights were made in clear-air turbulence for two speed and two weight conditions. Simultaneous acceleration measurements were taken at the center of gravity and at several stations along the wing span from which the true airplane acceleration was determined.

An analysis of the results indicated that the recorded center-of-gravity acceleration increments were, on the average, equal to the true airplane acceleration increment amplified by a factor of approximately 1.28 and further increased by approximately 0.01g. Within the accuracy of the results, there were no important changes in this relationship that could be attributed to variations in speed and weight.

## INTRODUCTION

In the flight operation of transport and bomber airplanes, atmospheric gusts constitute a principal source of loads. Knowledge of these loads is based primarily on V-G type of records and other acceleration measurements taken in the fuselage near the center of gravity of the airplane and interpreted on the basis that the airplane acts as a rigid body. For some of the newer and larger airplanes, interpretation of acceleration measurements on a rigid body basis may lead to errors attributable to the effect of transient wing response in gusts. The results of a flight investigation made on a two-engine transport airplane in rough air (ref. 1) have shown that, for the case investigated,

the use of fuselage accelerations in evaluating gust measurements can lead to errors, averaging about 20 percent.

Two principal effects of transient wing response on center-of-gravity acceleration measurements exist. One is a vibratory effect due to the excitation by the gusts of the natural modes of vibration of the airplane which causes the acceleration measured at the center of gravity to differ from the true airplane acceleration. The other is an aerodynamic effect due to the fact that the transient response causes a change in the total aerodynamic load that acts on the airplane. When vibratory response of the wing is important, therefore, center-of-gravity acceleration measurements may not be adequate for gust studies.

In order to establish the magnitude of transient-response effects on an airplane of a different configuration than that reported in reference 1 and to provide data suitable for comparison with transient-response calculations being made, a flight investigation was undertaken on a four-engine bomber airplane at Langley Field, Va. Acceleration, strain, and wing-twist measurements were made at a number of spanwise stations during flights through clear-air turbulence for two speeds and two weight conditions. The primary purpose of the present paper was to investigate the effects of wing vibration on center-of-gravity acceleration measurements. In addition, an estimate was made of the change in total aerodynamic load associated with transient response, and possible methods of evaluating or obtaining acceleration data free of vibratory effects were considered.

#### APPARATUS AND TESTS

The characteristics of the test airplane are given in table I and a three-view line drawing is given in figure 1. The estimated spanwise stiffness distribution, using EI as a measure of local wing stiffness, is shown in figure 2. The estimated spanwise weight distribution exclusive of fuel is shown in figure 3(a). The limits of the fuel load distributions of all runs are shown in figures 3(b) and 3(c) for the wing-heavy and wing-light fuel conditions, respectively.

The primary instrumentation for the investigation reported herein consisted of an NACA recording accelerometer mounted near the center of gravity and several remote recording electrical accelerometer units mounted at a number of stations along the wing span. The locations, types, and natural frequencies of all accelerometers used are given in figure 4. The electrical accelerometer units were located as close as feasible to the elastic axis of the wing as determined from the

manufacturer's ground-vibration tests. The accelerometer units at station 278 were located as close as practicable to the nodal points of the fundamental bending mode of the wing on the basis of ground-vibration tests. Dual instrumentation was used at station 278 on both left and right wings so that separate and electrically combined recordings of left- and right-wing nodal accelerations could be made. (The combined recording gives an average value of acceleration from the left- and right-wing nodal points and should exclude effects of antisymmetrical motion.) NACA attitude recorders were located at the stations shown in figure 4 in order to obtain a measure of the twist of the wing with reference to the fuselage station. A standard NACA airspeed-altitude recorder was used to obtain a record of airspeed and altitude and an NACA  $\frac{1}{2}$ -second chronometric timer was used to correlate all records.

The tests consisted of a series of runs, each approximately 50 miles in length, at different weights and speeds, in clear rough air. The different weight conditions are due entirely to variations in fuel load. The two weight conditions in these tests were for fuel loads corresponding to wing-heavy and wing-light conditions (see fig. 3). Four runs were made on each flight, two at a forward speed of approximately 250 miles per hour and two at approximately 180 miles per hour. The measured accelerations, for a given level of turbulence, were expected to be considerably lower than those in the previous investigation (ref. 1) primarily because of a higher wing loading of the airplane used in these tests. In view of the lower accelerations expected, two flights were made for each of the two weight conditions to obtain more accurate results for the range of accelerations measured. The flight conditions for the runs reported herein are given in table II.

#### EVALUATION OF DATA

The records obtained and the evaluation of the data were very similar to those in reference 1. As in reference 1, the method of analysis consisted primarily in comparing the accelerations measured by an accelerometer near the center of gravity with the true airplane acceleration. The acceleration at the nodal point of the fundamental bending mode, with the effects of the higher modes taken into account by fairing, is assumed to be the true airplane acceleration.

Sections of the record in which the fundamental mode of vibration predominated were analyzed to determine the actual nodal point of the airplane wing in flight and to check on the validity of using the estimated nodal point (station 278). It was noted from the records, as would be expected, that the vibratory accelerations outboard of station 278 were  $180^\circ$  out of phase with those inboard of this station. The results

of an evaluation of several sections of the records are shown in figure 5 for the two wing-weight conditions where simultaneous acceleration measurements at various stations along the wing span have been normalized for an average unit tip acceleration (average of left- and right-tip accelerations). It is apparent from these results that for all weight conditions tested the estimated nodal point (station 278) can be considered the nodal point for the purpose of this paper.

Examination of the acceleration records for the nodal point (station 278) revealed that, in addition to accelerations which were attributed to gust and engine vibrations, vibratory accelerations of approximately 5 cycles per second were frequently present on both the single and electrically combined traces. These vibratory accelerations were, in general, approximately  $180^\circ$  out of phase on the left- and right-wing nodal acceleration histories and thus indicated an antisymmetrical mode. The same vibratory frequency was present on the electrically combined nodal acceleration histories because of differences in amplitude of vibration between the left and right wings. From inspection of the twist records, the 5-cycle-per-second vibration appeared to be a low-amplitude twist oscillation and, with few exceptions, was less than the accuracy of measurement. Hence, this vibration was not considered significant in the analysis. The nodal-point acceleration traces were therefore faired as illustrated in figure 6 when such vibrations were present. Also shown in figure 6 is a time history of the center-of-gravity acceleration trace with the corresponding faired nodal-point trace superimposed for purposes of comparison.

If transient wing response were not present, acceleration measurements at the center of gravity and at the nodal points should be the same. On the basis that transient-response effects were superimposed on the airplane accelerations, the effects of transient wing response were eliminated from the records by fairing and the results were used as a check on the accuracy of instrumentation and on techniques employed in determining nodal-point accelerations. These results are shown in figure 7 where the electrically combined nodal-point acceleration measurements are shown as a function of the separate nodal accelerations and as a function of the center-of-gravity accelerations in which the effect of all vibratory modes has been eliminated by fairing. The three techniques are seen to be in good agreement. In checking nodal-point position and methods of nodal acceleration measurement, samples of the records from all accelerometers were used. However, only center-of-gravity and electrically combined nodal acceleration measurements are used for the remaining acceleration evaluation.

Records of center-of-gravity acceleration increments and corresponding nodal acceleration increments were available for analysis from four runs in each speed and weight condition. On each of the available

runs, sufficient gust accelerations were evaluated to provide a description of the data. As an example, the data for one run are presented in figure 8 in which the center-of-gravity acceleration increments are plotted as a function of the nodal-point acceleration increments (electrically combined). Since the trend of the data is roughly linear, least-squares solutions for a straight line fitted to the test points are used to describe the data and are presented in figure 8 as dashed lines. The straight lines fitted to the data do not always pass through the origin since the measured accelerations at the center of gravity include effects of engine vibration and higher mode vibrations which appear to be independent of the acceleration magnitude.

Examination of the records from the attitude recording instruments indicated that the incremental wing twist at the two outboard stations (stations 452 and 806) due to the gusts experienced in the test was less than  $\pm 0.1^\circ$ , or approximately within the accuracy of the twist measurements. The effect of wing twist, if present, is estimated to change the aerodynamic load due to gusts by no more than 3 percent. Since the effect of wing twist on acceleration measurements is indicated to be small and showed no consistent variation with load, it is not considered further.

#### PRECISION

In the analysis of the flight acceleration records, both peak (maximum indication including vibrations) and faired readings were made. Consideration of the character of the records, repeatability of the readings, and accuracy of the instrumentation leads to the belief that errors are less than  $\pm 0.05g$  for peak type of readings and less than  $\pm 0.10g$  when fairing is employed in the evaluation. The accuracy of the recording attitude gyroscopes used for wing twist measurements is estimated to be within  $\pm 0.10^\circ$  for a single gust.

#### RESULTS AND DISCUSSION

Descriptions of the available data were obtained by the least-squares solution for a straight line  $\Delta n_{cg} = K_1 + K_2 \Delta n_{nodal}$ , where  $\Delta n_{cg}$  is the acceleration increment at the center of gravity,  $K_1$  is the offset at the origin,  $K_2$  is the amplification factor, and  $\Delta n_{nodal}$  is the acceleration increment at the nodal point. Although the data from a single run are not believed to be sufficient to provide an adequate description of dynamic-response effects (because of low maximum acceleration values and few points at the high values on any one run),

least-squares solutions and the corresponding standard errors for all runs are given in table II to show the scatter of the data. Least-squares solutions and standard errors for the positive and negative accelerations treated separately and combined without regard to sign are given in table II as well as the average weight, average altitude, and acceleration-increment level for each run. (The acceleration-increment level is given as the absolute average of the highest positive and negative acceleration increments experienced during the run.) Representative data from each run in the same test condition were combined to obtain the most reliable description of dynamic-response effects for each condition and the least-squares solutions and standard errors for these data are given in table III.

The scatter of the amplification factor  $K_2$  for the individual-run data shown in table II is rather large. The amplification factor for the positive and negative acceleration data, combined without regard to sign, is shown in figure 9 as a function of the acceleration-increment level for each run. Although the data shown in figure 9 indicate that the amplification factors are, in general, higher for the runs with the larger acceleration values, insufficient data are available to establish definite conclusions.

Data from all runs in the same test condition (from which the values of table III were obtained) are plotted in figures 10(a) and 10(b) for the wing-light and wing-heavy conditions, respectively. From the descriptions of the data in table III it is evident that the values of the offset  $K_1$ , having an average value of about 0.01g, are sufficiently small to be neglected in the present investigation. Some differences appear between the amplification factors for the various conditions (table III and fig. 10), but in making comparisons of the data for speed and weight effects, the only difference of any consequence appears between the amplification factors for the 250- and the 180-mile-per-hour data of the wing-light condition. Statistical analysis indicated that this difference was greater than could be attributed to scatter of the data. This difference, although not altogether borne out by the wing-heavy condition, would indicate a small effect of speed, the higher amplification factors being associated with the higher speed. No differences were found in the data that could be attributed to variations in the test weight of the airplane. Within the accuracy of the data, an average amplification factor of 1.28 with an average offset of 0.01g applies for all the test conditions. This description of the data is shown by the dashed lines in figure 10 for purposes of comparison.

In addition to causing a difference between the fuselage accelerations and the nodal-point accelerations, transient response may cause an appreciable change in the total aerodynamic load on the airplane. The change in aerodynamic load due to wing response in the fundamental bending

mode was calculated by use of strip theory on the basis of the mode shape shown in figure 5 and the estimated fundamental wing frequencies from the flight records (table I). The results of the calculations, which neglected unsteady-lift effects, indicate that the net change in aerodynamic load due to this mode of vibration would result in airplane accelerations of  $\pm 0.02g$  or less when the vibratory fuselage acceleration was  $\pm 0.30g$ . Thus, the change in total aerodynamic load due to this mode of vibration is relatively small.

The available data for runs at 250 miles per hour were analyzed on the basis of the time (or distance) required to reach the maximum value of acceleration for any gust, since current theory indicates that transient-response effects vary with this parameter. The time from the intersection of the acceleration trace with the  $1g$  reference to the subsequent acceleration peak was utilized for this analysis, and, for simplicity, is hereinafter referred to as "time-to-peak acceleration." For transient-response calculations, some assumptions are made as to the initial conditions on entry into a gust and as to the variation of the gust velocity from start to peak. Repeated gusts, variations in gust shape, and spanwise gust effects are present in the flight data and may obscure any variation of transient response with time-to-peak acceleration. However, in order to determine whether such a relationship exists, the available data were sorted into three groups according to time-to-peak acceleration. The medians of the groups were approximately 0.15 second, 0.40 second, and 0.75 second. About 40 percent of the data were associated with the median time-to-peak acceleration of 0.40 second (approx. 12 chord lengths travel for a flight speed of 250 mph) with the remainder of the data divided equally between the other two groups. Least-squares solutions were obtained for straight lines fitted to the data, and the amplification factor  $K_2$  obtained by this means is plotted in figure 11 as a function of the median value of time-to-peak acceleration in each group for the wing-light and the wing-heavy conditions. The results shown in figure 11 indicate that the transient response effects are greater when the time-to-peak acceleration is small.

In view of the differences between fuselage and nodal acceleration measurements, methods of evaluating or obtaining acceleration measurements free of vibratory effects have been investigated. The results used to check the instrumentation and techniques (fig. 7) indicate that, as found in reference 1, the faired fuselage measurements are satisfactory for estimating airplane acceleration. Where the vibratory accelerations can be distinguished from the accelerations due to gusts, this method of fairing fuselage accelerations would seem to provide an adequate measure of true airplane acceleration. This method would be applicable for gust studies provided the aerodynamic and torsional effects of wing flexibility were small. Inasmuch as fairing of the records may not



always be feasible because of cramped or reduced time scales, the use of combined nodal-point accelerometers has been proposed as a method of measurement. An evaluation of this method was made and the results are shown in figure 12. Peak readings from the electrically combined nodal accelerometers are plotted as a function of the nodal-point accelerations (true airplane acceleration) in which acceleration effects of higher modes, when present, have been eliminated by fairing. It can be seen that the acceleration difference (on the basis of the least-squares solution which is shown as a dashed line) is about one-half of that when peak fuselage measurements were used. Although some of the difference noted may be due to response of the instrument to engine vibration, the major part appeared to be due to secondary wing vibration.

#### CONCLUDING REMARKS

A flight investigation was undertaken on a four-engine bomber airplane to determine the effect of transient wing response in rough air upon acceleration measurements at the center of gravity of the airplane. For the airplane tested, the results showed that in rough air the maximum or peak recorded acceleration increment at the center of gravity was, on the average, equal to the true airplane acceleration increment amplified by a factor of approximately 1.28 and further increased by a constant value of approximately 0.01g. (This compares with 1.20 and 0.05g as determined from the previous investigation on a two-engine transport airplane.) There was an indication that the amplification factor increased with magnitude of acceleration, but this relationship could not be substantiated. Within the accuracy of determination, the differences between fuselage and nodal accelerations were not affected by variations in weight and only slightly affected by variations in speed covered by the test conditions. This relationship is in substantial agreement with results obtained from the previous flight investigation.

The results of an analysis indicated that transient-response effects on total aerodynamic load would be small for the test airplane. An analysis of the data on the basis of time-to-peak acceleration indicated that the largest transient-response effects were associated with the accelerations having the smallest time-to-peak values.

The results also indicated that the vibratory effects of wing flexibility can be compensated for in time-history acceleration measurements at the center of gravity by fairing the fundamental and higher wing frequencies. Peak readings from an electrical combination of left- and right-wing nodal acceleration measurements gave a better measure of

the acceleration of the airplane than peak center-of-gravity acceleration measurements, although not so good as faired center-of-gravity measurements.

Langley Aeronautical Laboratory  
National Advisory Committee for Aeronautics  
Langley Field, Va., April 21, 1952

#### REFERENCE

1. Shufflebarger, C. C., and Mickleboro, Harry C.: Flight Investigation of the Effect of Transient Wing Response on Measured Accelerations of a Modern Transport Airplane in Rough Air. NACA TN 2150, 1950.

TABLE I  
CHARACTERISTICS OF TEST AIRPLANE

Span, feet . . . . .	141.2
Mean aerodynamic chord, feet . . . . .	12.9
Wing area, square feet . . . . .	1,739
Slope of lift curve, per radian . . . . .	5.04
Aspect ratio . . . . .	11.6
Center-of-gravity position, percent M.A.C. . . . .	(approx.) 22
Fundamental frequency, wing bending (ground vibration tests, no fuel condition), cycles per second . . . . .	3.3
Estimated fundamental wing frequency from flight records, wing- heavy condition, cycles per second . . . . .	2.8
Estimated fundamental wing frequency from flight records, wing- light condition, cycles per second . . . . .	3.0



TABLE II  
FLIGHT CONDITIONS AND LINEAR DESCRIPTION OF DATA

Run	Flight condition			Least-squares solution and standard errors, $\Delta n_{cg} = K_1 + K_2 \Delta n_{nodal}$					
	Average weight, lb	Average altitude, ft	Acceleration-increment level, g units (*)	Offset, $K_1$ , g units			Amplification factor, $K_2$		
				Positive data	Negative data	Combined data	Positive data	Negative data	Combined data
(a) Wing-light condition									
Speed, 250 mph									
1	93,000	2,600	0.39	0.01 ± 0.01	-0.01 ± 0.01	0.01 ± 0.01	1.20 ± 0.04	1.25 ± 0.06	1.23 ± 0.03
2	89,000	2,400	.34	.01 ± .01	.01 ± .01	.00 ± .01	1.17 ± .04	1.31 ± .06	1.27 ± .04
3	92,000	2,500	.68	.01 ± .01	-.03 ± .01	.01 ± .01	1.43 ± .03	1.20 ± .04	1.34 ± .03
4	90,000	2,300	.45	.03 ± .01	-.04 ± .01	.03 ± .01	1.31 ± .05	1.24 ± .05	1.28 ± .03
Speed, 180 mph									
1	91,000	2,500	0.30	0.03 ± 0.01	0.01 ± 0.01	0.02 ± 0.01	1.07 ± 0.05	1.30 ± 0.05	1.17 ± 0.04
2	90,000	2,300	.23	.00 ± .01	-.02 ± .01	.01 ± .01	1.17 ± .05	1.12 ± .08	1.12 ± .04
3	91,000	2,200	.49	.04 ± .01	-.02 ± .01	.03 ± .01	1.17 ± .04	1.22 ± .03	1.19 ± .03
4	90,000	2,000	.37	.04 ± .01	-.01 ± .01	.03 ± .01	1.27 ± .04	1.23 ± .06	1.24 ± .04
(b) Wing-heavy condition									
Speed, 250 mph									
1	105,000	2,200	0.35	0.03 ± 0.01	-0.05 ± 0.01	0.04 ± 0.01	1.17 ± 0.05	1.22 ± 0.08	1.17 ± 0.05
2	101,000	3,000	.35	.02 ± .02	-.03 ± .01	.03 ± .01	1.26 ± .11	1.14 ± .07	1.18 ± .07
3	106,000	1,700	.43	.02 ± .01	.00 ± .01	.01 ± .01	1.24 ± .05	1.47 ± .05	1.32 ± .03
4	102,000	1,200	.53	.02 ± .01	-.01 ± .01	.02 ± .01	1.24 ± .04	1.50 ± .04	1.33 ± .03
Speed, 180 mph									
1	103,000	3,400	0.26	0.01 ± 0.01	0.02 ± 0.01	0.00 ± 0.01	1.17 ± 0.06	1.36 ± 0.07	1.23 ± 0.05
2	102,000	3,000	.26	.03 ± .02	-.02 ± .01	.03 ± .01	1.02 ± .12	1.26 ± .08	1.10 ± .08
3	104,000	1,500	.41	.02 ± .01	-.02 ± .01	.02 ± .01	1.28 ± .05	1.22 ± .05	1.25 ± .03
4	103,000	1,000	.29	.01 ± .01	-.02 ± .01	.01 ± .01	1.39 ± .06	1.25 ± .06	1.31 ± .05

\*Average of highest positive and negative nodal acceleration increments, disregarding sign.



TABLE III

## LINEAR DESCRIPTION OF DATA FOR TEST CONDITIONS

Weight condition	Speed, mph	Least-squares solution and standard errors, $\Delta n_{cg} = K_1 + K_2 \Delta n_{nodal}$					
		Offset, $K_1$ , g units			Amplification factor, $K_2$		
		Positive data	Negative data	Combined data	Positive data	Negative data	Combined data
Wing-light	250	$0.00 \pm 0.01$	$-0.02 \pm 0.01$	$0.01 \pm 0.01$	$1.37 \pm 0.02$	$1.25 \pm 0.02$	$1.31 \pm 0.02$
	180	$.02 \pm .01$	$.00 \pm .01$	$.01 \pm .01$	$1.21 \pm .03$	$1.26 \pm .02$	$1.23 \pm .02$
Wing-heavy	250	$0.02 \pm 0.01$	$-0.01 \pm 0.01$	$0.02 \pm 0.01$	$1.22 \pm 0.02$	$1.44 \pm 0.03$	$1.30 \pm 0.02$
	180	$.01 \pm .01$	$-.02 \pm .01$	$.01 \pm .01$	$1.30 \pm .03$	$1.25 \pm .03$	$1.28 \pm .02$

NACA

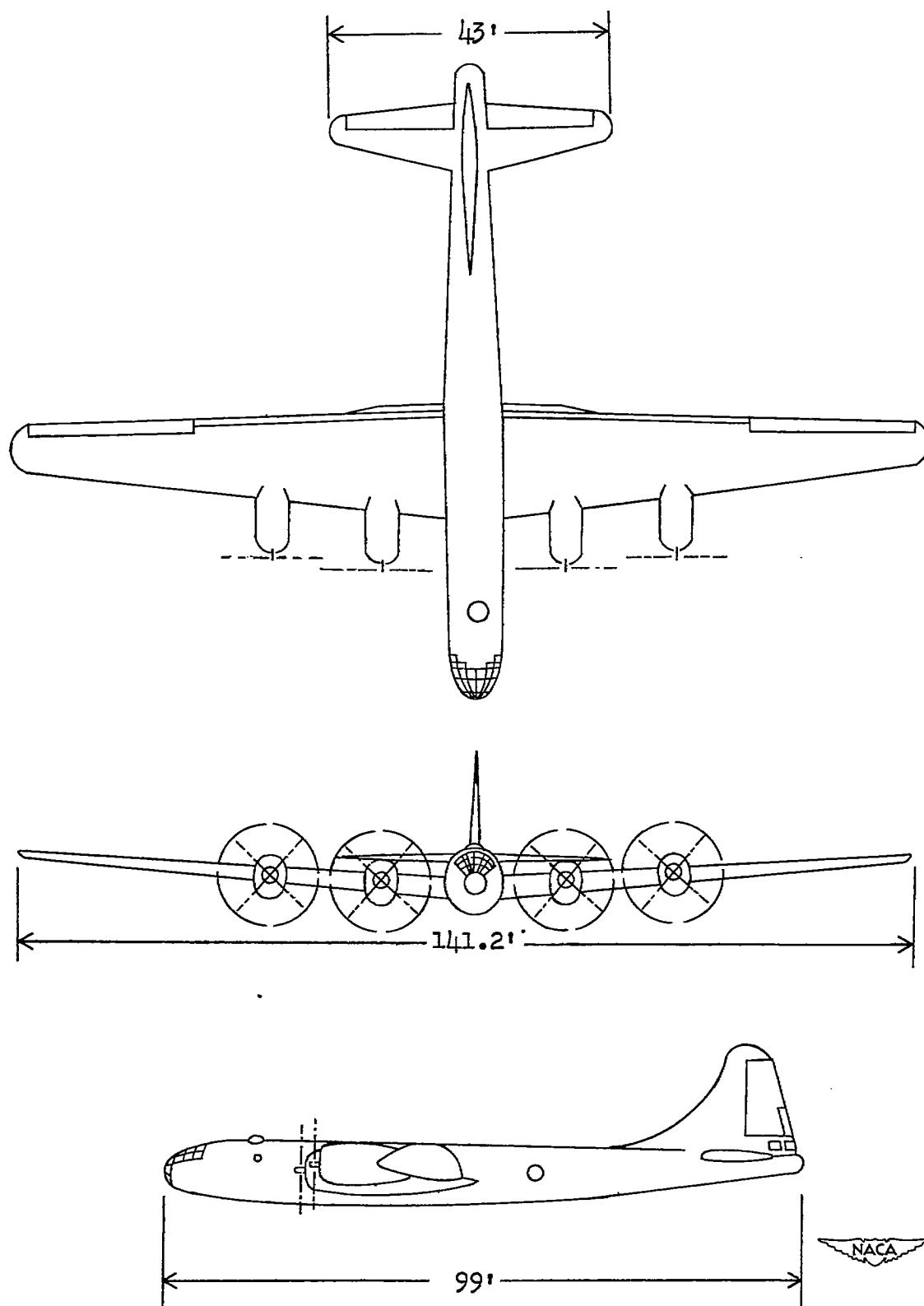


Figure 1.- Three-view drawing of test airplane.

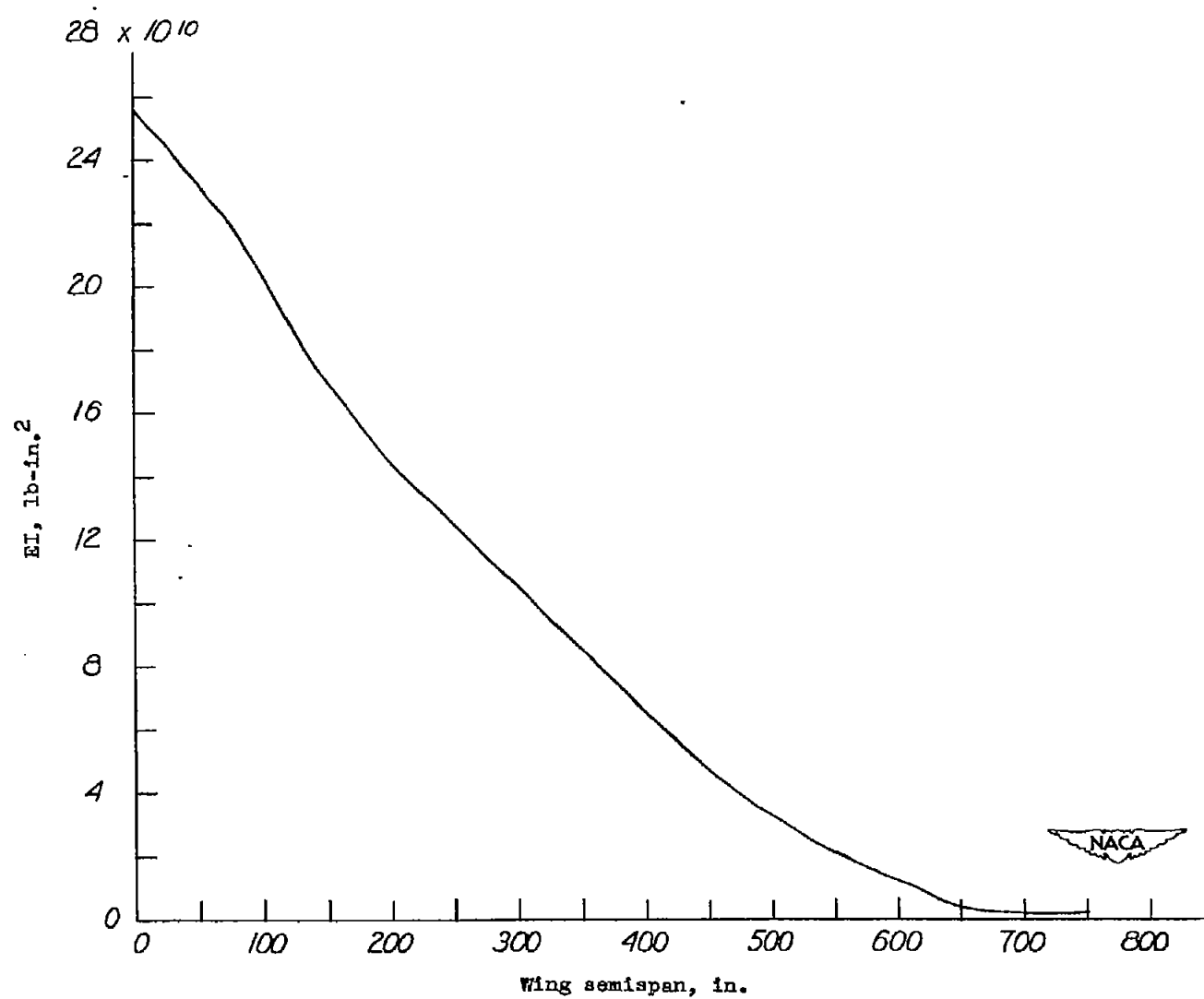
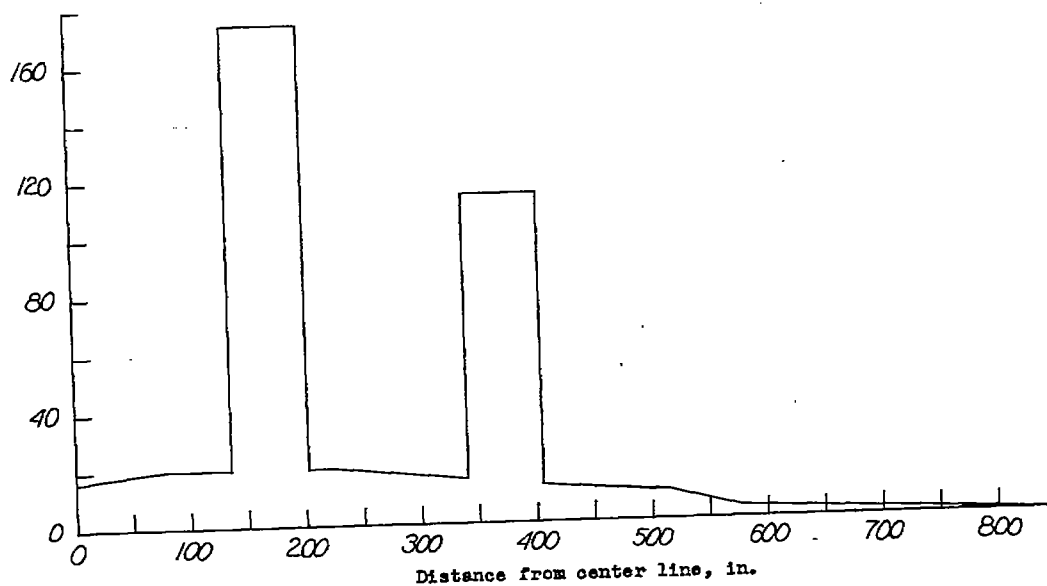
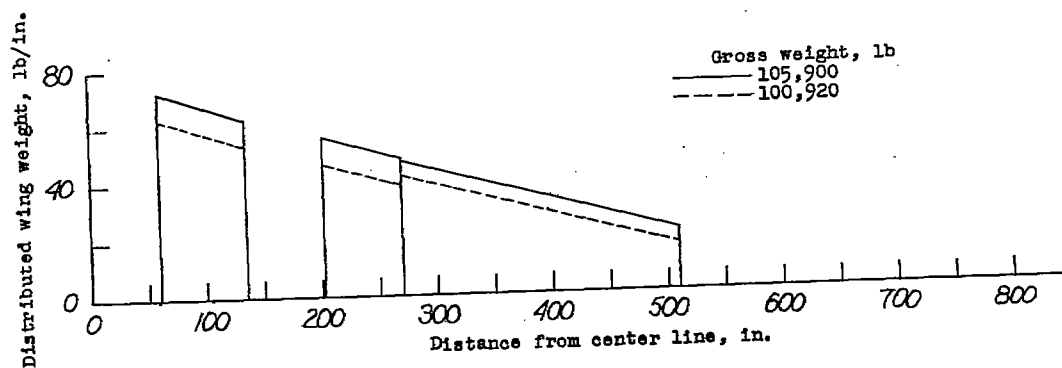


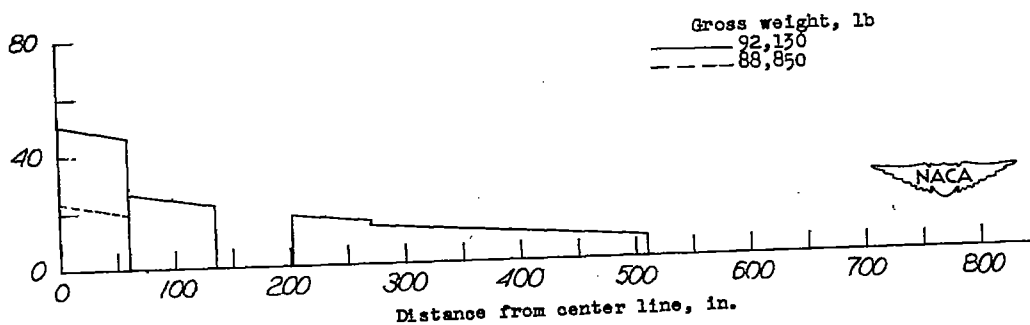
Figure 2.- Estimated spanwise stiffness distribution.



(a) Wing structure and nacelles.



(b) Fuel load, wing-heavy condition.



(c) Fuel load, wing-light condition.

Figure 3.- Estimated spanwise wing weight distribution.



	Type of accelerometer	Natural frequency, cps
○	Statham, electrical	45 or greater
□	NACA, optical	13.5
△	NACA, electrical	16.0

◇ NACA attitude recorder (twist)

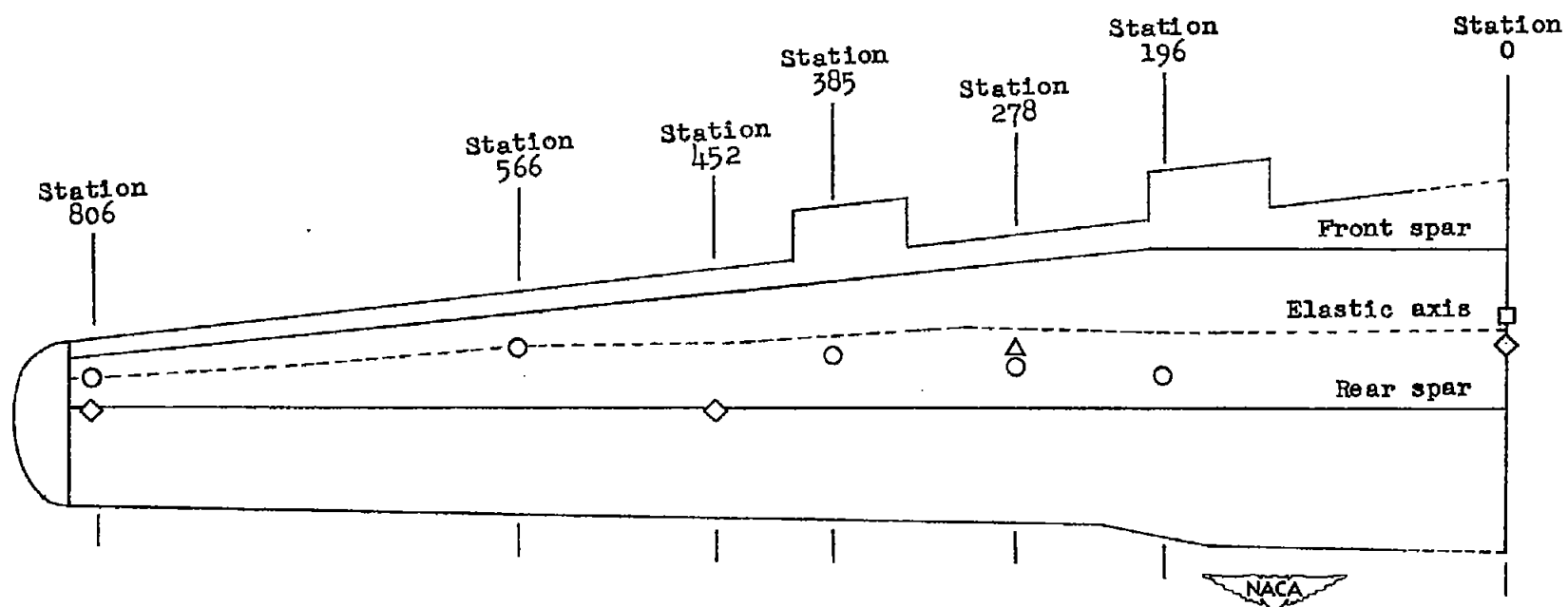


Figure 4.- Accelerometer and attitude-recorder locations in left wing of test airplane. (Accelerometer installations at station 278 and station 806 were repeated in right wing.)

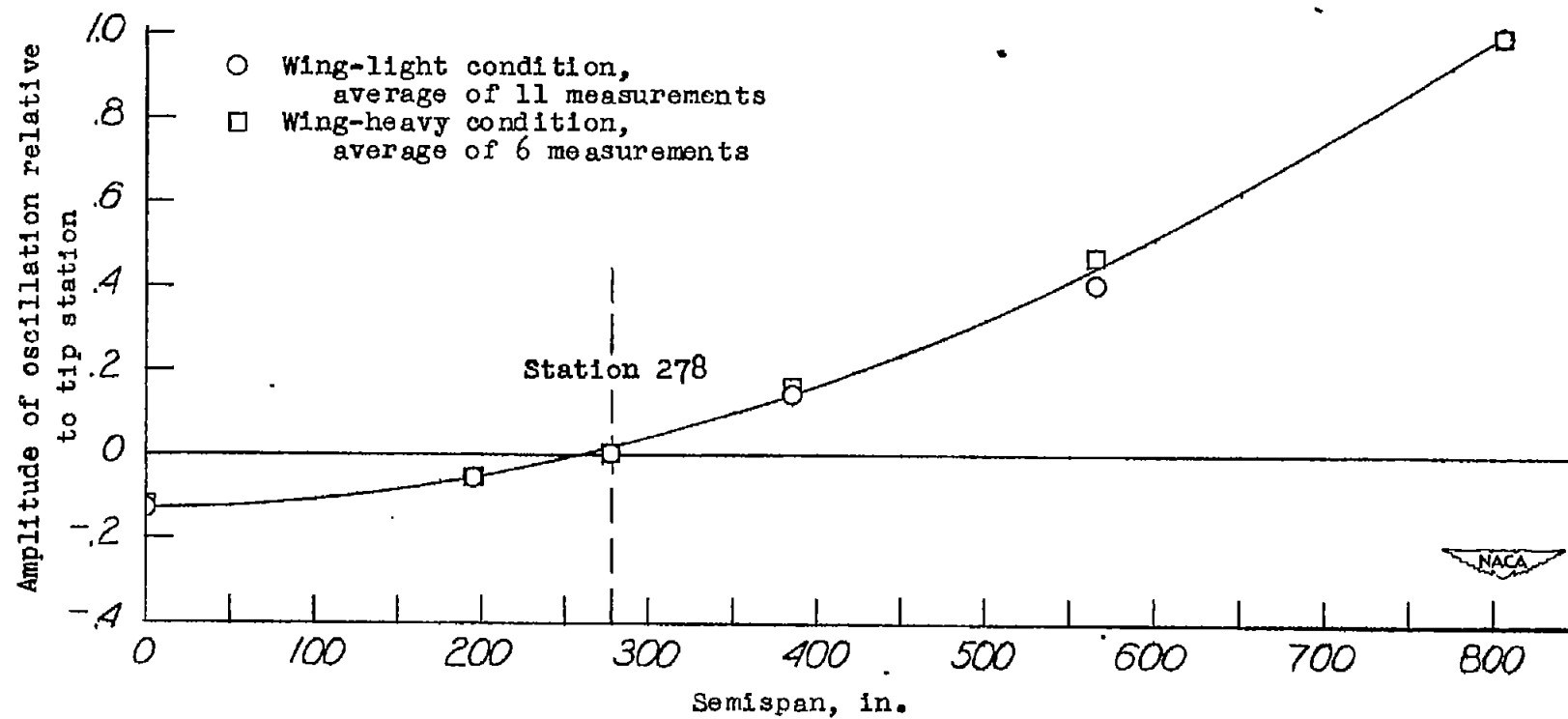
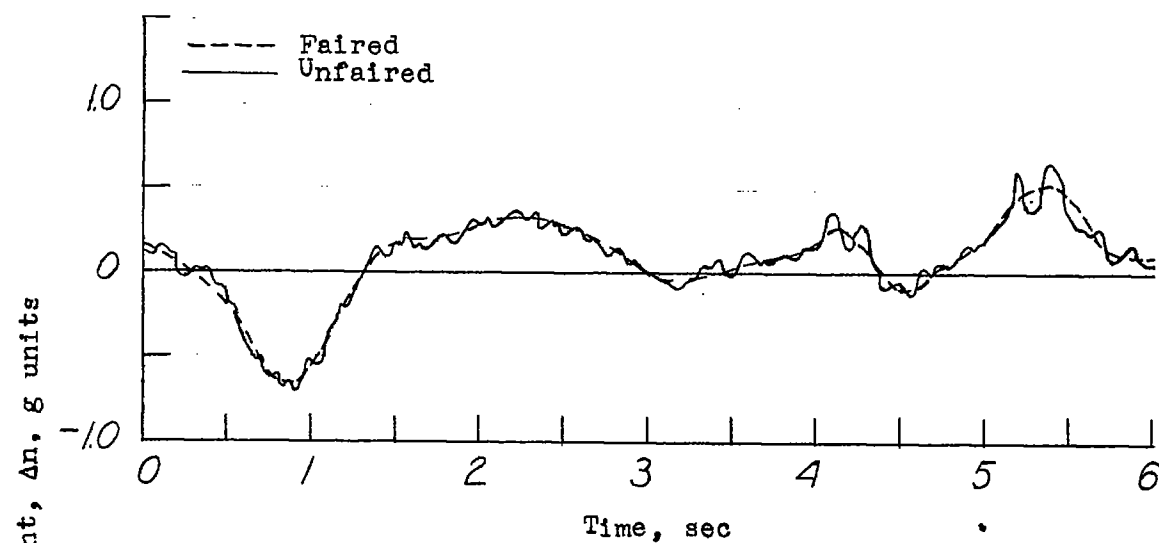
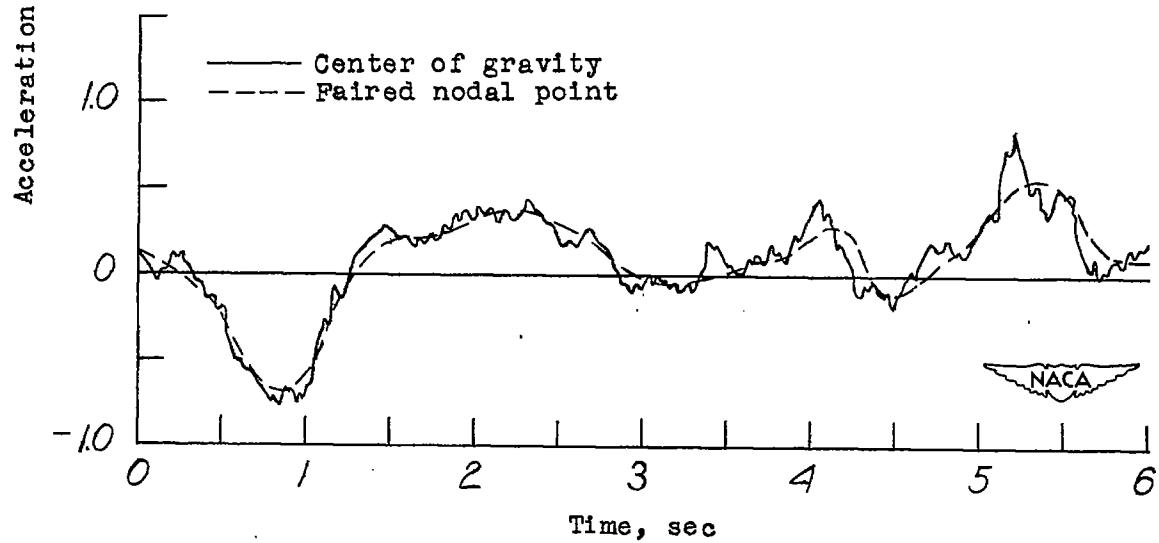


Figure 5.- Location of nodal point from accelerometer flight records.



(a) Nodal points (electrically combined).



(b) Center of gravity compared with faired nodal point.

Figure 6.- Time history of acceleration in gust.

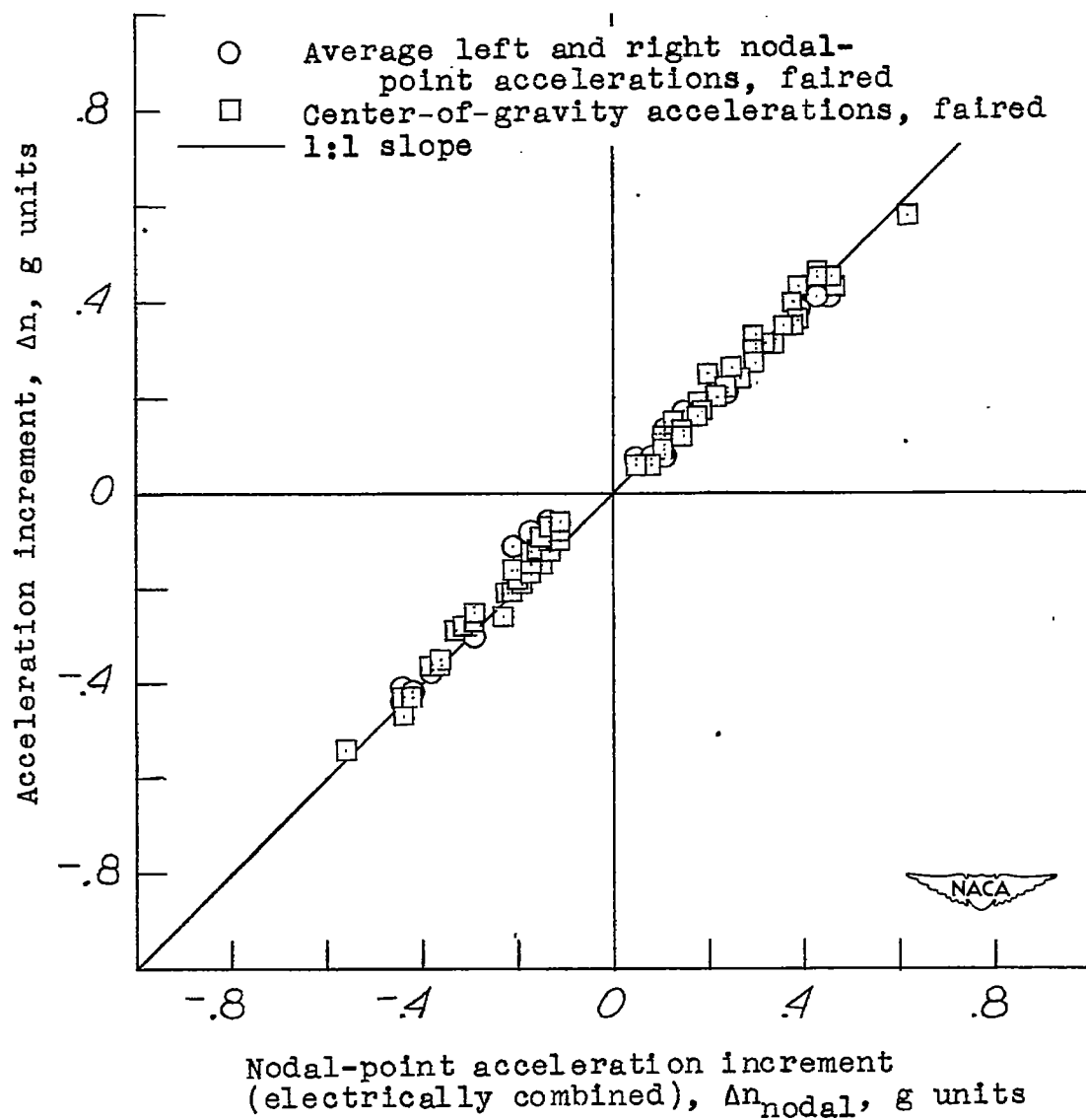


Figure 7.- Comparison of means of determining nodal-point acceleration.

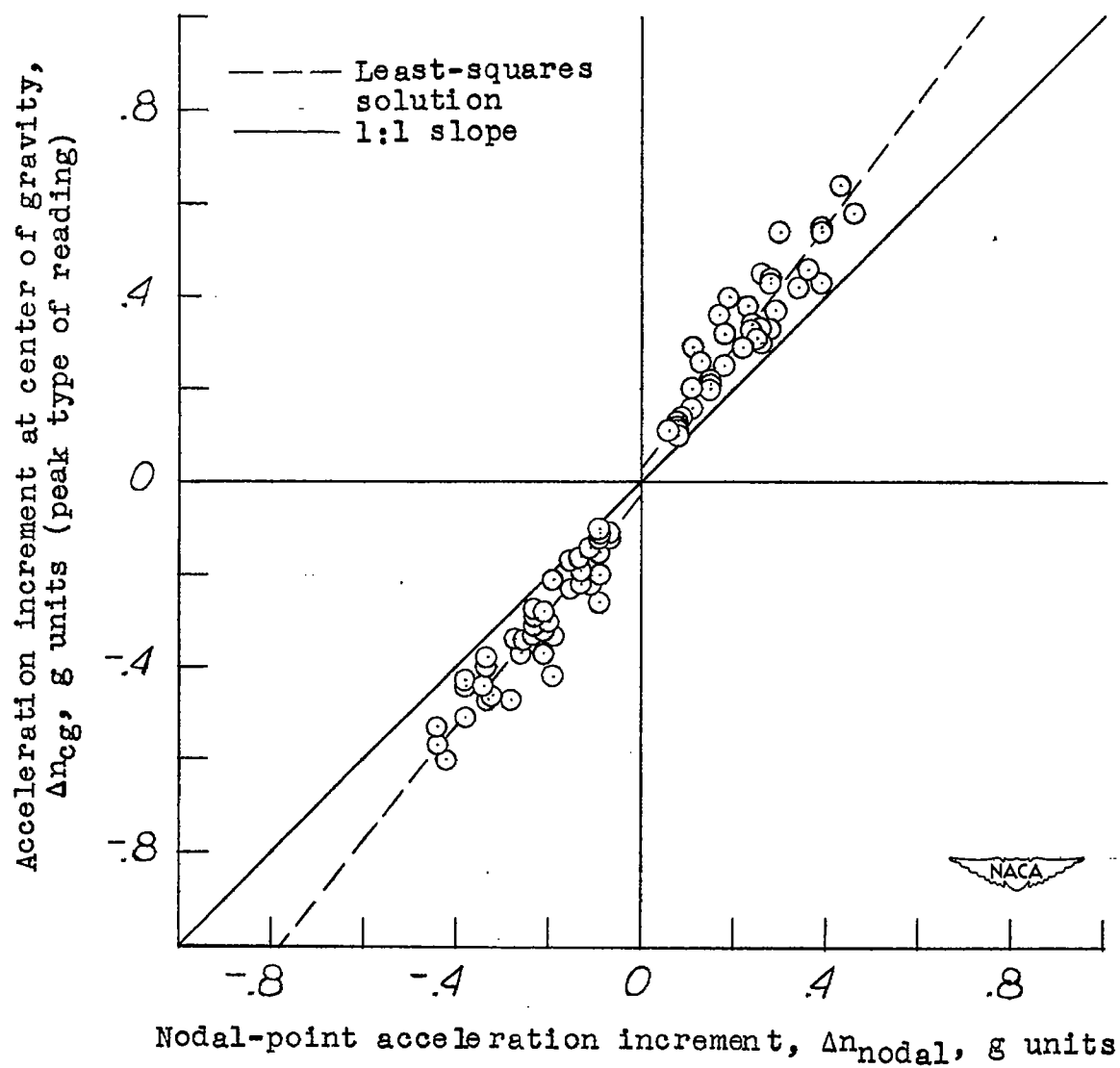


Figure 8.- Acceleration at center of gravity as a function of average nodal-point acceleration. (Sample run.)

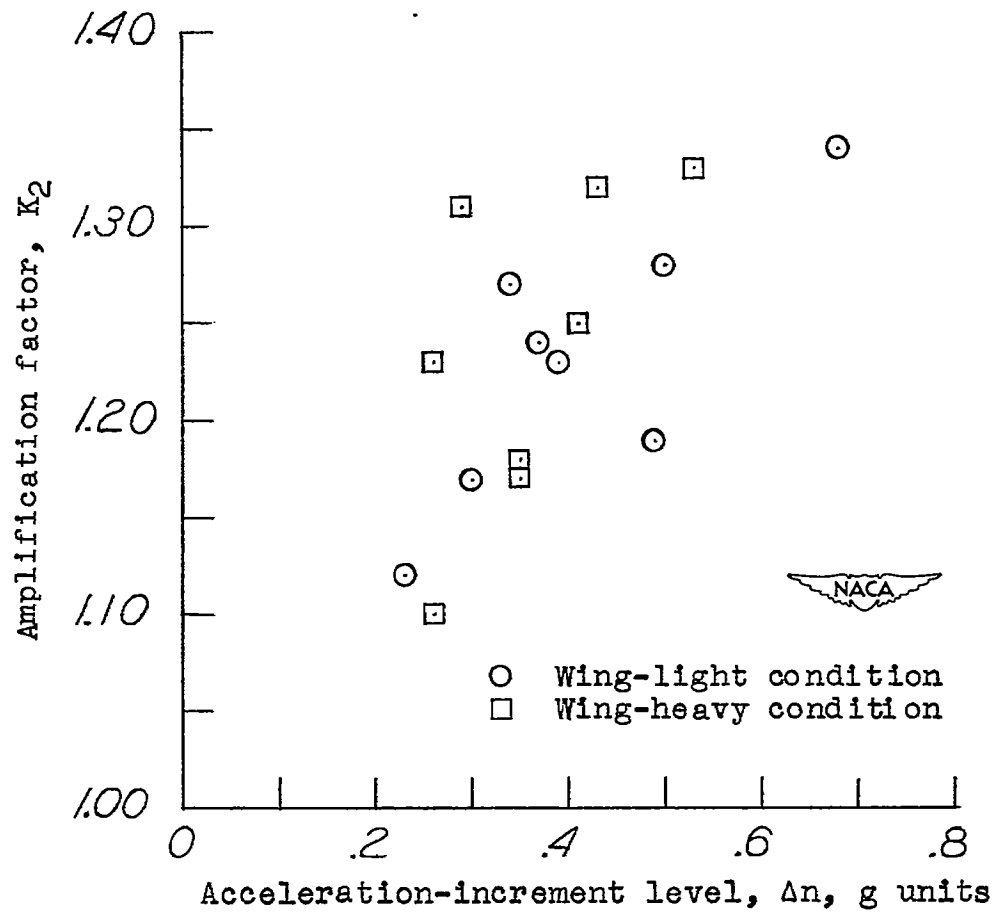
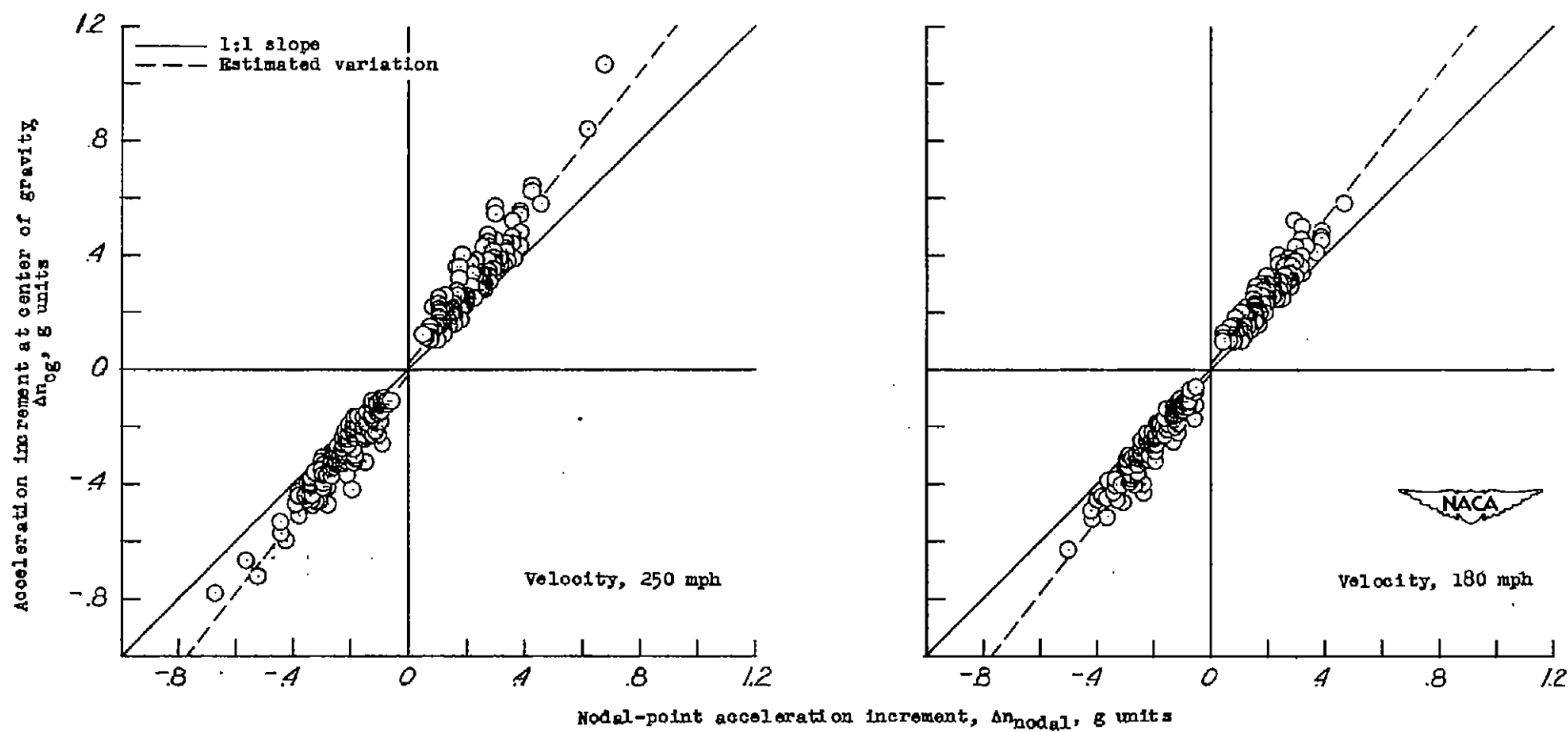
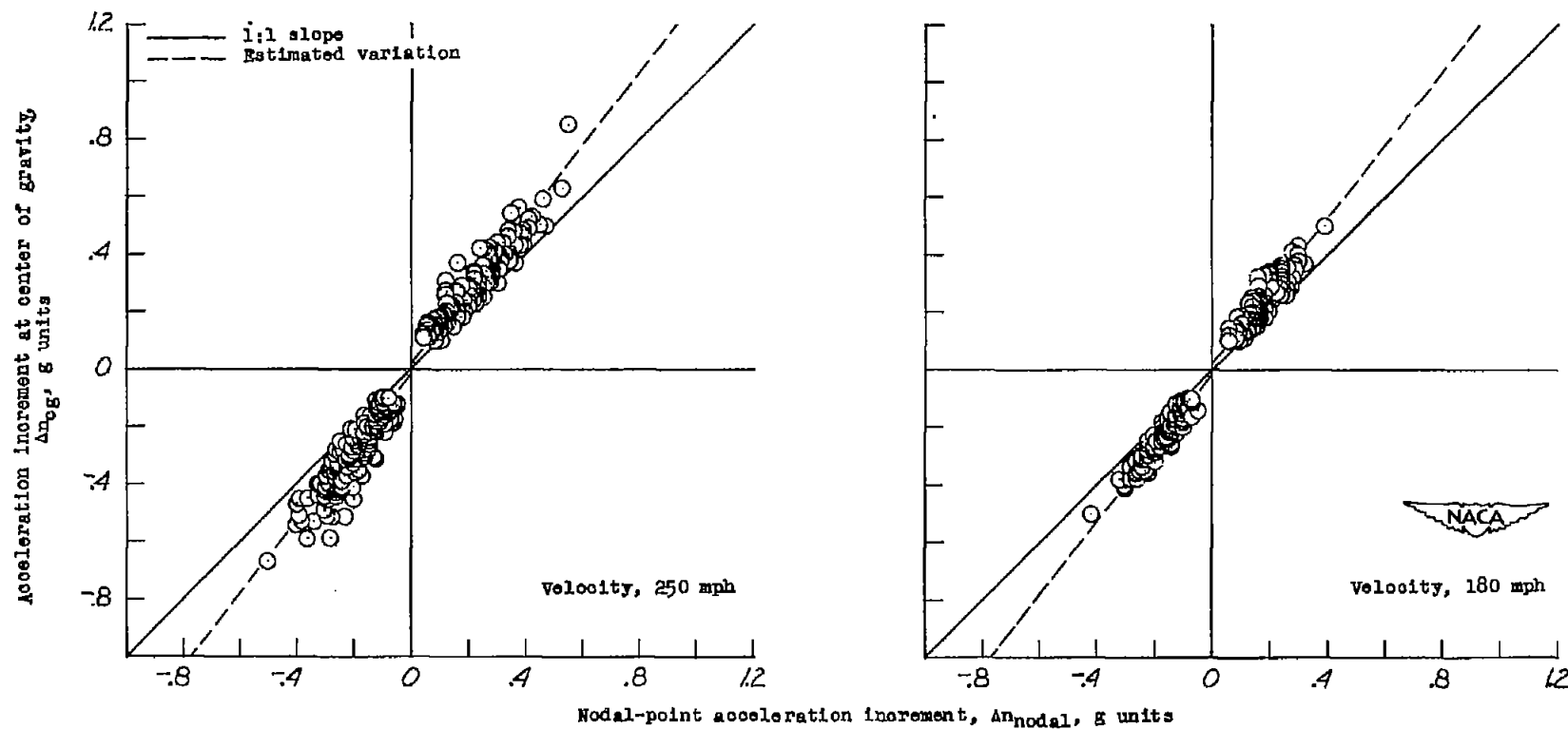


Figure 9.- Variation of amplification factor with acceleration-increment level.



(a) Wing-light condition.

Figure 10.- Acceleration at center of gravity as a function of average nodal-point acceleration.



(b) Wing-heavy condition.

Figure 10.- Concluded.



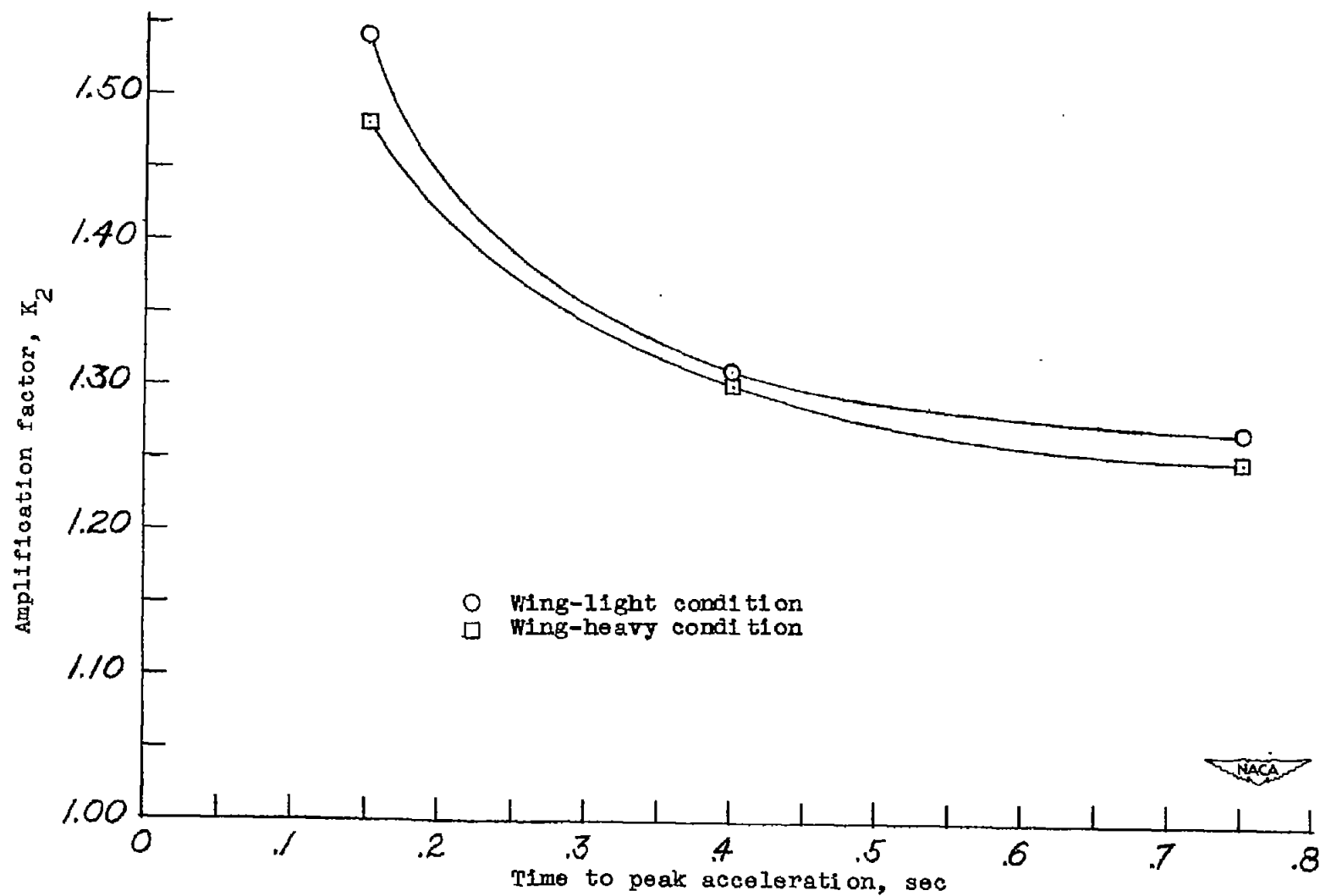


Figure 11.- Amplification factor as a function of time to peak acceleration. (250-mph data.)

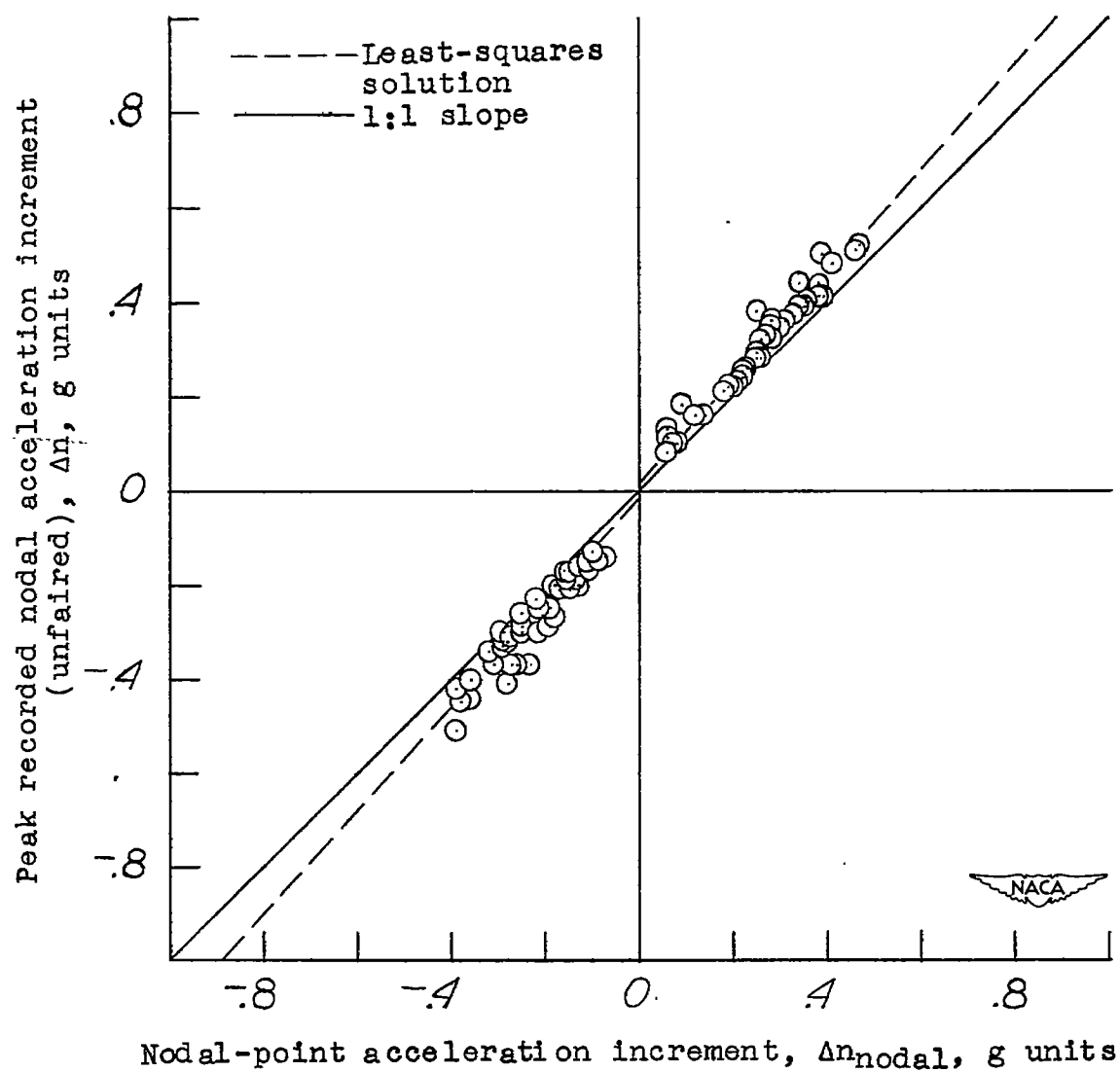


Figure 12.- Peak recorded nodal accelerations (unfaired) as a function of nodal-point accelerations.